Proceedings of The ASME 2018 Dynamic Systems and Control Conference
DSCC 2018
Sept. 30-Oct. 3, 2018, Atlanta, Georgia, USA

ASME2018/DSCC2018-9061

HUMAN-INSPIRED ALGEBRAIC CURVES FOR WEARABLE ROBOT CONTROL

Alireza Mohammadi
Dept. Bioengineering and Dept. Mechanical Engineering
The University of Texas at Dallas
Richardson, Texas 75080
Email: alireza.mohammadi@utdallas.edu

Robert D. Gregg
Dept. Bioengineering and Dept. Mechanical Engineering
The University of Texas at Dallas
Richardson, Texas 75080
Email: rgregg@utdallas.edu

ABSTRACT

Having unified representations of human walking gait data is of paramount importance for wearable robot control. In the rehabilitation robotics literature, control approaches that unify the gait cycle of wearable robots are more appealing than the conventional approaches that rely on dividing the gait cycle into several periods, each with their own distinct controllers. In this article we propose employing algebraic curves to represent human walking data for wearable robot controller design. In order to generate algebraic curves from human walking data, we employ the 3L fitting algorithm, a tool developed in the pattern recognition literature for fitting implicit polynomial curves to given datasets. For an impedance model of the knee joint motion driven by the hip angle signal, we provide conditions by which the generated algebraic curves satisfy a robust relative degree condition throughout the entire walking gait cycle. The robust relative degree property makes the algebraic curve representation of walking gaits amenable to various nonlinear output tracking controller design techniques.

INTRODUCTION

Wearable robot control and biomechanical gait assessment require compact and reduced order representations of human walking data during the entire gait cycle. In the rehabilitation robotics literature, wearable robot controllers that aim at unifying the entire human gait cycle [1–8] are more preferable to the conventional control schemes [9–13] that rely on dividing the gait cycle into several periods, each with their own distinct controllers. State-of-art wearable robot control techniques that rely on non-unified representations of walking gait result in dozens of control parameters and transition rules that must be tuned across users and activities [13]. Furthermore, desynchronizing perturbations increase a patient's risk of falling if the controller switches to the wrong state and as a result uses the wrong control scheme.

Unified gait wearable robot controllers do not suffer the aforementioned shortcomings of the non-unified gait control schemes. In [1], the authors employed the center of pressure (COP) in human walking to unify the stance phase of the gait. Assuming a rocker foot geometry, the COP-based gait in [1] only depends on the joint variable measurements, as opposed to the joint velocities. Therefore, the COP-based gait is a *holonomic* representation of human walking gait. A unified holonomic gait, which unifies the stance and swing phases of walking, was proposed in [14]. The unified gait in [14], however, uses the patient's absolute coordinates in order to measure phase variables and thus requires using motion capture systems.

In order to unify the stance and swing phases of human walking, the authors in [4, 5] departed from the COP-based holonomic gaits to a thigh angle integral-based representation of human walking. However, the integral term in [4, 5] needs to be reset at the beginning of every gait cycle to prevent accumulation of drift due to variation in thigh kinematics. Furthermore, the integral-based gait in [4,5] cannot be used for patient's non-rhythmic motion control. The authors in [8] and [15] have proposed a piecewise holonomic representation of human walking gait cycle and a unified velocity-based (nonholonomic) gait representation, respectively. The authors in [16] employed a symbolic algebraic tool, which is based on computing resultant of polynomials, for

removing phase variables from *autonomous bipedal robot* parametric gaits. However, this approach cannot be *practically* used for generating closed algebraic curves from human walking data due to *large degrees* of generated implicit polynomials. A unified holonomic representation of human gait cycle, which unifies both the stance phase and the swing phase during walking, is still lacking in the literature.

In this article we propose employing closed algebraic curves to represent human walking data for wearable robot controller design. The closed curve representation of human walking data is holonomic and motivated by the fact that healthy hip-knee time profiles create closed and non-intersecting orbits during walking in the hip-knee plane (see Figure 1). Such closed-curve representations of human walking data have numerous wearable robot applications such as synchronization control between the patient's hip and powered knee prosthesis in above-knee amputees, as well as path-based approaches for patient gait training using lower limb exoskeletons [17, 18].

In order to generate algebraic curves from human walking data, we provide bivariate implicit polynomials (IPs) whose zero sets represent the nominal coordination between the hip and knee angles during normal level walking. Furthermore, we employ the 3L fitting algorithm [19], a tool developed in the pattern recognition literature for fitting implicit polynomial curves to given datasets, for obtaining algebraic curves from human data. Moreover, we prove that there exists *no holonomic relationship* between the hip angle signal and the knee joint angle that possesses a well-defined relative degree throughout the entire gait cycle. This result is *independent* of the method by which the unified holonomic gait is generated from the human walking data. Finally, we provide conditions by which the generated algebraic curves satisfy a robust relative degree condition, as defined in [20], for an impedance model of the knee joint motion driven by the hip angle signal throughout the entire walking gait cycle. The robust relative degree property, despite the loss of relative degree at some singular points during the gait cycle, makes the algebraic curve representation of walking gaits amenable to nonlinear output tracking controller design [21].

We remark that our proposed algebraic curve fitting is closely related to the recent work in [18], where the authors use an elliptical path in the hip-knee plane to prescribe a normal walking gait for a lower limb exoskeleton during the swing phase. Our algebraic curve representation, however, unifies the entire gait cycle, including both the stance phase and the swing phase. Furthermore, unlike the elliptical path in [18], which is an open curve converging to infinity, our proposed algebraic curves are closed and bounded, which correspond to periodic human gait cycles. The closed and bounded curve properties cannot be achieved with standard one dimensional polynomial fitting numerical methods, similar to the one used in [18].

The rest of this paper is organized as follows. First, we briefly review preliminaries from algebraic curves and present the 3L algorithm for fitting such curves to nominal hip-knee human walking data. Next, for an impedance model of the knee joint motion driven by the hip angle signal, we provide conditions by which the generated algebraic curves satisfy a robust relative degree condition throughout the entire gait cycle. Finally, we conclude the paper with final remarks and outline of possible future research directions.

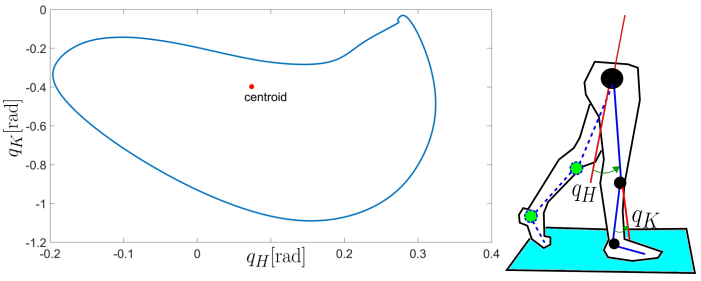

(a) (b)

Figure 1: (a) Nominal human hip-knee path taken from Winter's normal cadence walking data [22]. (b) The body diagram of the walking sagittal plane: q_H and q_K represent the hip and knee angles, respectively.

3L ALGORITHM FOR FITTING HUMAN DATA TO ALGEBRAIC CURVES

In this section we briefly review some preliminaries on algebraic curves and use the 3L algorithm for fitting closed algebraic curves to human data. A comprehensive treatment of algebraic curves and their properties may be found in [23–25].

Algebraic Curves

Algebraic curves are defined by means of bivariate implicit polynomials (IPs). Given a finite integer n, an IP $h(q_H, q_K)$ is a function

$$h(q_H, q_K) = \sum_{ij} a_{ij} q_H^i q_K^j,\ 0 \le i+j \le n \tag{1}$$

of the two variables q_H, q_K, where a_{ij} are real numbers.

The *degree of the polynomial* $h(q_H, q_K)$ in (1) is the maximal value of $i+j$ for which $a_{ij} \neq 0$. Here, we assume that the IP h is of degree n. Every IP of degree n has a total of $(n+1)(n+2)/2$ coefficients.

Given an IP $h(q_H, q_K)$ and a point (q_{H_0}, q_{K_0}), the value $h(q_{H_0}, q_{K_0})$ is called the *algebraic distance* of the point (q_{H_0}, q_{K_0}) to the zero set of $h(q_H, q_K)$. Moreover, the *zero set* of the IP $h(q_H, q_K)$ given by (1) is defined to be

$$\mathcal{Z}(h) := \left\{ (q_H, q_K) \in \mathbb{R}^2 \middle| h(q_H, q_K) = 0 \right\}. \tag{2}$$

A *real algebraic curve* is the zero set of a non-zero real bivariate polynomial h. The *degree of an algebraic curve* is defined to be the degree of its associated bivariate implicit polynomial. Algebraic curves of degree 1, 2, 3, 4, $\cdots$, are called *lines*, *conics*, *cubics*, *quartics*, $\cdots$, respectively. Ellipses, hyperbolas and parabolas are examples of well-known conics.

Since we are interested in studying periodic human walking gait profiles, it is desirable to have closed and bounded algebraic curves. The following well-known lemma from the algebraic curve literature provides the necessary condition for a given algebraic curve to be closed and bounded.

Lemma 1.([25]) *An algebraic curve is a closed and bounded plane curve only if it is of even degree.*

3L Algorithm for Fitting Algebraic Curves to Human Walking Data

In this section we fit algebraic curves to the data points obtained from a healthy gait according to Winter's normal cadence walking data [22]. Our fitting algorithm is taken from the pattern recognition literature and is known as the 3L algorithm [19]. We first describe how fitting algebraic curves to human walking datasets can be formulated as a quadratic optimization problem.

Fitting algebraic curves to human datasets as a quadratic optimization problem. Consider an ordered, closed set, $\mathcal{H}_0$, of N_0 planar data points (q_{H_i}, q_{K_i}). Here, the set $\mathcal{H}_0$ represents the path in the hip-knee plane, which is taken from the Winter's normal cadence walking data [22] (see Figure 1). The set of ordered data points (q_{H_i}, q_{K_i}), $1 \leq i \leq N_0$, are the samples of the hip and knee normal cadence walking trajectories corresponding to increasing time instants during a given gait cycle. In other words, if (q_{H_i}, q_{K_i}) corresponds to time instant t_i and $(q_{H_{i+1}}, q_{K_{i+1}})$ corresponds to time instant t_{i+1}, then $t_i < t_{i+1}$. Since the walking gait profile is periodic, we have $(q_{H_1}, q_{K_1}) = (q_{H_{N_0}}, q_{K_{N_0}})$. The geometric center or centroid of the dataset $\mathcal{H}_0$ is defined to be the point (see also Figure 1)

$$C = \begin{bmatrix} q_{HC} \\ q_{KC} \end{bmatrix} := \begin{bmatrix} \frac{\sum_{i=1}^{N_0-1} q_{Hi}}{N_0-1} \\ \frac{\sum_{i=1}^{N_0-1} q_{Ki}}{N_0-1} \end{bmatrix}. \tag{3}$$

We would like to find an implicit bivariate polynomial $h(q_H, q_K)$ of even degree, i.e., $n = 2p$ for some positive integer p, such that its zero set $\mathcal{Z}(h)$ approximates the set of human hip-knee data points $\mathcal{H}_0$. This approximation problem is equivalent to minimization of the error functional [19]

$$E = \sum_{(q_H, q_K) \in \mathcal{H}_0} h^2(q_H, q_K). \tag{4}$$

It is possible to describe the error functional E in (4) as a quadratic function of the coefficients of the IP $h(q_H, q_K)$. In order to do so, we rewrite the IP $h(q_H, q_K) = \sum_{ij} a_{ij} q_H^i q_K^j$, where $0 \leq i + j \leq n$, using the inner-product

$$h(q_H, q_K) = m^\top(q_H, q_K) a, \tag{5}$$

where

$$\begin{aligned} m^\top(q_H, q_K) := \big[& 1, q_H, q_K, q_H^2, q_H q_K, q_K^2, \cdots, q_H^n, \\ & q_H^{(n-1)} q_K, q_H^{(n-2)} q_K^2, \cdots, q_H q_K^{(n-1)}, q_K^n \big], \end{aligned} \tag{6}$$

is a function of the two variables q_H and q_K. Moreover,

$$\begin{aligned} a := \big[& a_{00}, a_{10}, a_{01}, a_{20}, a_{11}, a_{02}, \cdots \\ & a_{n0}, a_{(n-1)1}, a_{(n-2)2}, \cdots, a_{1(n-1)}, a_{0n} \big], \end{aligned} \tag{7}$$

is the vector of IP coefficients with

$$n_0 := (n+1)(n+2)/2, \tag{8}$$

components. Next, using the data points $(q_{H_i}, q_{K_i}) \in \mathcal{H}_0$, $1 \leq i \leq N_0$, we define the following matrix

$$M_{\mathcal{H}_0} := \begin{bmatrix} m_1^\top \\ \cdots \\ m_{N_0}^\top \end{bmatrix}, \tag{9}$$

where the row vectors $m_i^\top$ are defined as $m_i^\top := m^\top(q_{H_i}, q_{K_i})$. It is shown in [19] that the functional E given by (4) is equal to

$$E = a^\top M_{\mathcal{H}_0}^\top M_{\mathcal{H}_0} a. \tag{10}$$

Therefore, we would like to find the coefficient vector a such that the error functional E given by (10) is minimized. The direct minimization of the quadratic error function E, which is known as the 1L approach, often fails to generate an acceptable IP fit to a set of data points due to numerical instability problems and/or lack of physically meaningful solutions (see [19, 26] for

a detailed discussion on numerical issues associated with this fitting approach).

Human data 3L fitting algorithm. Using the 3L fitting algorithm developed in [19], we address the aforementioned numerical shortcomings of the 1L minimization by introducing two additional datasets, which can be generated from the original human walking dataset $\mathcal{H}_0$. Being able to vary the two fictitious datasets on either side of the original normal cadence walking dataset $\mathcal{H}_0$, optimal fitting accuracies of algebraic curves to human walking data can be achieved. Furthermore, it can be shown that, under suitable conditions, the algebraic curves generated by the 3L fitting algorithm are non-degenerate [19, 27, 28].

Following the experimental results for pose estimation in computer graphics literature [19, 25], we chose quartic algebraic curves, i.e., $n = 4$, to be fitted to the hip-knee normal walking data. However, there is no limitation on the degree of the algebraic curve that can be fitted to human walking datasets. The 3L algorithm for fitting algebraic curves to human hip-knee walking data can be described in the following three steps.

Step 1) Generation of two fictitious datasets: Given the dataset $\mathcal{H}_0$, representing the nominal human walking gait in the hip-knee plane [22], introduce two fictitious datasets close to $\mathcal{H}_0$. The first set, which is denoted by $\mathcal{H}_+$ and is located outside the dataset $\mathcal{H}_0$, has N_+ points and corresponds to the algebraic distance c (see the previous section for the definition of algebraic distance), where c is a design parameter to be chosen. The second fictitious dataset, which is denoted by $\mathcal{H}_-$ and is located inside the dataset $\mathcal{H}_0$, has N_- points and corresponds to the algebraic distance $-c$. In this article, we have chosen the algebraic distance design parameter to be $c = 1$.

In order to generate the two fictitious datasets $\mathcal{H}_+$ and $\mathcal{H}_-$ in this article, we translated the centroid or the geometric center of the dataset $\mathcal{H}_0$ given by (3) to the origin of the $q_H - q_K$ plane. In particular, we translated the original dataset to obtain

$$\mathcal{H}_0^t = \left\{ \begin{bmatrix} q_H \\ q_K \end{bmatrix} - \begin{bmatrix} q_{HC} \\ q_{KC} \end{bmatrix} : \begin{bmatrix} q_H \\ q_K \end{bmatrix} \in \mathcal{H}_0 \right\}, \tag{11}$$

where $[q_{HC}, q_{KC}]^\top$ is the centroid of the human dataset $\mathcal{H}_0$.

Then, we scaled the translated dataset $\mathcal{H}_0^t$ by scaling factors α_+ and α_-, where α_+ is a real number greater than 1 and α_- is a real number less than 1, to generate $\mathcal{H}_+$ and $\mathcal{H}_-$, respectively. The multiplication of the translated dataset $\mathcal{H}_0^t$ by α_+ and α_- corresponds to *geometric contraction* and *geometric dilation*, respectively. Therefore,

$$\mathcal{H}_\pm = \left\{ \alpha_\pm \Big(\begin{bmatrix} q_H \\ q_K \end{bmatrix} - \begin{bmatrix} q_{HC} \\ q_{KC} \end{bmatrix} \Big) : \begin{bmatrix} q_H \\ q_K \end{bmatrix} \in \mathcal{H}_0 \right\}. \tag{12}$$

For the presented results, we chose $\alpha_+ = 1.02$ and $\alpha_- = 0.98$.

Remark 1. *In Steps 2 and 3, we consider $\mathcal{H}_0^t$ and $\mathcal{H}_\pm$ in* (11) *and* (12)*, respectively, whose geometric centers are located at the origin of the $q_H - q_K$ plane. In the final step, the generated algebraic curve needs to be translated back to the geometric center of human dataset $\mathcal{H}_0$.* △

Step 2) Defining the three level-set matrix: Define the three level-set (3L) matrix

$$M_{3L} := \begin{bmatrix} M_{\mathcal{H}_-} \\ M_{\mathcal{H}_0^t} \\ M_{\mathcal{H}_+} \end{bmatrix} \in \mathbb{R}^{(N_+ + N_0 + N_-) \times n_0}, \tag{13}$$

where n_0 is the number of coefficients of the IP h given by (8). In (13), the matrices $M_{\mathcal{H}_0^t}$, $M_{\mathcal{H}_+}$, and $M_{\mathcal{H}_-}$ are defined as

$$M_{\mathcal{H}_0^t} := \begin{bmatrix} m^\top(q_{H_1}^t, q_{K_1}^t) \\ \cdots \\ m^\top(q_{H_{N_0}}^t, q_{K_{N_0}}^t) \end{bmatrix}, M_{\mathcal{H}_\pm} := \begin{bmatrix} m^\top(q_{H_1}^\pm, q_{K_1}^\pm) \\ \cdots \\ m^\top(q_{H_{N_\pm}}^\pm, q_{K_{N_\pm}}^\pm) \end{bmatrix}, \tag{14}$$

where the points $(q_{H_i}^t, q_{K_i}^t)$, $1 \le i \le N_0$, belong to the dataset $\mathcal{H}_0^t$ given by (11). Similarly, the points $(q_{H_{i_\pm}}^\pm, q_{K_{i_\pm}}^\pm)$, $1 \le i \le N_\pm$, belong to the two fictitious datasets $\mathcal{H}_+$ and $\mathcal{H}_-$ given by (12), respectively.

Step 3) Solving for the unknown IP coefficients: Define the $(N_+ + N_0 + N_-)$ component column vector of algebraic distances

$$b := \begin{bmatrix} -c\mathbb{1}_{N_-} \\ 0\mathbb{1}_{N_0} \\ c\mathbb{1}_{N_+} \end{bmatrix}, \tag{15}$$

where $\mathbb{1}_k$, for a given integer k, is a column vector of ones belonging to $\mathbb{R}^k$. Consider the equation $M_{3L}a = b$, with M_{3L} given by (13) and b given by (15). Computing the pseudo-inverse solution for the coefficient vector a, we have

$$a^\star = \left(M_{3L}^\top M_{3L}\right)^{-1} M_{3L}^\top b.$$

The algebraic curve fitted to the human data is the zero set of

$$h^\star(q_H, q_K) = m^\top(q_H - q_{HC}, q_K - q_{KC})a^\star, \tag{16}$$

where $m^\top(\cdot,\cdot)$ is the function defined by (6), and $[q_{HC}, q_{KC}]^\top$ is the centroid of the human dataset $\mathcal{H}_0$. The translation in (16)

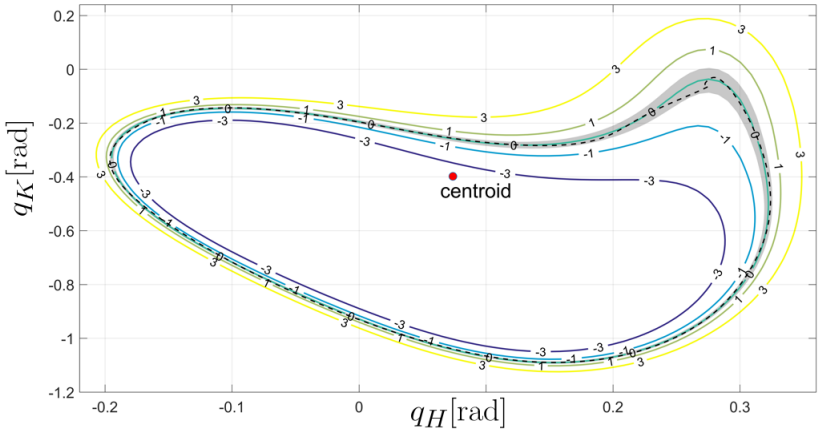

Figure 2: The quartic algebraic curve fitted to Winter's normal cadence walking data [22]. The dashed curve represents the Winter's normal cadence walking. The level sets of the IP $h^\star(q_H,q_K)$ are labeled with their corresponding algebraic distance in the figure. The green band around the zero set of the IP $h^\star(q_H,q_K)$ corresponds to the hip and knee configurations that belong to the sublevel set $\{(q_H,q_K) : |h^\star(q_H,q_K)| \leq c_0\}$ associated with the algebraic distance $c_0 = 0.3$.

corresponds to translation of the geometric center of the obtained algebraic curve from the origin to the human dataset centroid, as explained in Remark 1.

Discussion of the obtained algebraic curve fit. Using the 3L algorithm, we obtained a quartic IP with vector of coefficients

$$a^\star = [-4.6, 37.8, 30.5, -183.3, -38, 18.4, -492.2, -624.5, \\ -380.6, -26.0, 3725.5, 1307.3, 1344.1, 11.3, 55.6].$$

Figure 2 depicts the level sets of the IP $h^\star(q_H,q_K)$ which has been generated using the aforementioned 3L fitting algorithm. The largest deviation of the quartic algebraic curve fit from Winter's normal cadence walking data happens during the stance extension at the configuration $[0.2677 \text{ rad}, -0.081 \text{ rad}]^\top$ where the knee angle deviates from the nominal value by around 0.04 rad $\approx 2.3^\circ$.

The green band around the zero set of the IP $h^\star(q_H,q_K)$ corresponds to the hip and knee configurations that belong to the sublevel set $\{(q_H,q_K) : |h^\star(q_H,q_K)| \leq c_0\}$ associated with the algebraic distance $c_0 = 0.3$. As it can be seen from Figure 2, the level sets of the fitted IP $h^\star(q_H,q_K)$ do not intersect with each other, corresponding to the fact that the generated algebraic curve is non-degenerate. Furthermore, as the algebraic distances from the zero set $\mathcal{Z}(h^\star)$ change in a small manner, the joint angles do not deviate drastically from the nominal values. This continuity feature is desirable for controller design, since for small values of $|h^\star(q_H,q_K)|$ the hip-knee configurations are still close to the fitted algebraic curve.

RELATIVE DEGREE ANALYSIS OF UNIFIED HOLONOMIC REPRESENATION OF HUMAN GAIT CYCLE

In this section we consider an impedance model of the knee joint motion driven by the hip angle signal and analyze the relative degree of the human-inspired algebraic curves for this dynamical system. The human-inspired IP $h^\star(q_H,q_K)$ represents a desired implicit relationship between the human's hip angle and the wearable robot knee angle. As the human's hip angle $q_H(t)$ evolves with time, driving $h^\star(q_H(t),q_K)$ to zero via feedback corresponds to coordinating the motion of the knee with the hip during level walking according to the human walking closed curve in Figure 1. We remark that the algebraic curve given by the IP $h^\star(q_H,q_K)$ represents a *holonomic* relationship as it only depends on the joint angles q_H and q_K, as opposed to the joint angle velocities.

We assume that the knee joint motion is governed by an impedance model with a nonlinear output function $y = h^\star(q_H(t),q_K)$ given by the IPs fitted to human normal walking data. Moreover, we assume that the signals associated with human hip joint position $q_H(t)$, hip joint velocity $\dot{q}_H(t)$, and hip joint acceleration $\ddot{q}_H(t)$ are smooth and bounded. Under this assumption, we have the dynamics

$$\begin{aligned} M\ddot{q}_K + B\dot{q}_K + Kq_K &= u, \\ y &= h^\star(q_H(t),q_K), \end{aligned} \tag{17}$$

where u is the torque applied to the knee. Whenever the output $h^\star(q_H(t),q_K)$ is zero or sufficiently close to zero, the motion of the knee joint gets coordinated with the driving hip angle signal according to the human walking closed curve in Figure 1.

For the impedance model given by (17), we first prove that there exists no holonomic relationship between the hip angle signal and the knee joint angle that possesses a well-defined relative degree throughout the entire gait cycle. This result implies that using an exact input-output feedback linearizing controller, and for that matter a PD control law[i], is impossible for synchronizing the hip–knee motion with a unified holonomic output. We remark that the loss of relative degree is independent of the method by which the output $y = h^\star(q_H(t), q_K)$ is generated from the human walking data.

Proposition 1. *Consider the impedance model of the knee joint motion driven by the hip angle signal given by* (17)*. For any smooth output function $h^\star(\cdot)$ whose zero set is a bounded and closed curve, there exists a singular point on the zero set of $h^\star(\cdot)$ such that the output $y = h^\star(q_H, q_K)$ loses its relative degree for the dynamical system in* (17)*.*

Proof. Consider the output $y = h^\star(q_H, q_K)$ for the dynamical system in (17). Taking two derivatives of the output, the control input appears in the following way

$$\ddot{y} = \frac{1}{M}\frac{\partial h^\star}{\partial q_K}(q_H, q_K)u + (\star), \tag{18}$$

where $(\star)$ represents the sum of all the remaining terms. We prove that there exists at least one point (q_H^*, q_K^*) on the zero set of $h^\star(\cdot)$, i.e., $\mathcal{Z}(h^\star)$, such that

$$\frac{\partial h^\star}{\partial q_K}(q_H^*, q_K^*) = 0.$$

Since the zero set $\mathcal{Z}(h^\star)$ is a smooth, closed, and bounded curve, by a direct result of the *Theorem of Turning Tangents* [29, Section 1.7, p. 39], there exists at least one point (q_H^*, q_K^*) on the curve $\mathcal{Z}(h^\star)$ such that the perpendicular vector to it is parallel to the q_K axis. Since the perpendicular vector to $\mathcal{Z}(h^\star)$ is given by $[\partial h^\star/\partial q_H, \partial h^\star/\partial q_K]^\top$, we have $(\partial h^\star/\partial q_K)(q_H^*, q_K^*) = 0$. Thus, the relative degree of the output $h^\star(\cdot)$ is lost at (q_H^*, q_K^*). ■

Despite the loss of relative degree at some singular points during the walking gait cycle, it is still possible to design output tracking nonlinear controllers provided that the human-inspired outputs satisfy a *robust relative degree condition* at the points of singularity [20]. Following *the dynamic extension* procedure in [30, Section 5.4, p. 249], we add one integrator at the torque input u. That is, we let

$$u = \zeta, \;\; \dot{\zeta} = v. \tag{19}$$

In order to study the robust relative degree of the human-inspired IP $h^\star$ at the points of singularity, we define $x := [q_K, \dot{q}_K, \zeta]^\top$ and rewrite the augmented dynamical system given by (17) and (19) in the following standard control affine form

$$\begin{aligned} \dot{x} &= f(x) + g(x)u, \\ y &= h(q_H(t), q_K), \end{aligned} \tag{20}$$

where

$$f(x) := \begin{bmatrix} 0 & 1 & 0 \\ -\frac{K}{M} & -\frac{B}{M} & 1 \\ 0 & 0 & 0 \end{bmatrix} x, \; g(x) := \begin{bmatrix} 0 \\ 0 \\ 1 \end{bmatrix}.$$

For the dynamical system in (20), we first present the definition of robust relative degree, according to [20]. Next, we present the condition by which the human-inspired algebraic curve has robust relative degree at the points of singularity during a walking gait cycle.

Definition 1 ([20]). *Consider the dynamical system in* (20)*. The human-inspired algebraic curve $\mathcal{Z}(h^\star)$ is said to have robust relative degree γ at $x = x_0$ if there exist smooth functions $\phi_i(x)$, $i = 1, \cdots, \gamma$, such that*

$$\begin{aligned} h^\star(x) &= \phi_1(x), \\ L_{f+gu}\phi_i(x) &= \phi_{i+1}(x) + \psi_i(x,u), \; i = 1, \cdots, \gamma - 1 \\ L_{f+gu}\phi_\gamma(x) &= b(x) + a(x)u + \psi_\gamma(x,u) \end{aligned}$$

where $L_{f+gu}\phi_i(x) := (\partial\phi_i/\partial x)(f(x) + g(x)u)$, and the functions $\psi_i(x)$, $i = 0, \cdots, \gamma$, are sums of terms of order $O(x)^2$, $O(x,u)$, or $O(u)^2$ at x_0 (denoted $O(x,u)^2$)[ii]. Furthermore, the functions $a(x)$ and $b(x)$ are smooth, and $a(x_0) \neq 0$.

The following proposition provides the condition by which the human-inspired algebraic curve satisfies a robust relative degree condition at singularities during the walking gait cycle.

Proposition 2. *Consider the impedance model of the knee joint motion driven by the hip angle signal, which is augmented with the integrator* (19)*, given by* (20)*. Suppose that the zero set of the smooth output function $h^\star(\cdot)$, i.e., $\mathcal{Z}(h^\star)$, is a bounded and closed curve. Consider the singular point(s) on the zero set $\mathcal{Z}(h^\star)$ where the output $y = h^\star(q_H, q_K)$ loses its relative degree. The output function $h^\star(\cdot)$ has robust relative degree $\gamma = 3$, with input $u = \zeta$ and output $y = h^\star(q_H, q_K)$, if*

$$\frac{\partial^2 h}{\partial q_K^2}\dot{q}_K + \frac{\partial^2 h}{\partial q_K \partial q_H}\dot{q}_H \neq 0 \tag{21}$$

[i] See, e.g., [1] for further details on using PD control schemes in place of input-output feedback linearizing controllers.

[ii] We say that a function $f(x)$ is of order $O(x)^2$ at $x = x_0$ if $\lim_{x \to x_0} \|f(x)\|/\|x - x_0\|^2$ exists and is not equal to zero.

at the points of singularity.

Proof. For the sake of brevity, we provide a sketch of the proof. Taking two derivatives of the output $y = h^{\star}(q_H, q_K)$, we have

$$\ddot{y} = \frac{1}{M}\frac{\partial h^{\star}}{\partial q_K}(q_H, q_K)u + \{\frac{\partial^2 h}{\partial q_K^2}\dot{q}_K + 2\frac{\partial^2 h}{\partial q_K \partial q_H}\dot{q}_H - \frac{B}{M}\frac{\partial h}{\partial q_K}\}\dot{q}_K + (\star\star),$$

where $(\star\star)$ represents the sum of all the remaining terms. Taking another derivative of the output, it can be seen that

$$\dddot{y} = \frac{1}{M}\{2\frac{\partial^2 h}{\partial q_K^2}\dot{q}_K + 2\frac{\partial^2 h}{\partial q_K \partial q_H}\dot{q}_H - \frac{B}{M}\frac{\partial h}{\partial q_K}\}u + (\star\star\star).$$

where $(\star\star\star)$ represents the sum of all the remaining terms, which is also independent of the control input u. Therefore, the output $y = h^{\star}(q_H, q_K)$ has robust relative degree $\gamma = 3$, with respect to the output of the integrator $u = \zeta$, if

$$2\frac{\partial^2 h}{\partial q_K^2}\dot{q}_K + 2\frac{\partial^2 h}{\partial q_K \partial q_H}\dot{q}_H - \frac{B}{M}\frac{\partial h}{\partial q_K} \neq 0.$$

Noting that at the points of singularity we have $\frac{\partial h}{\partial q_K} = 0$ (see the proof of Proposition 1), we conclude that the robust relative degree holds if the inequality in (21) is satisfied at these singular points. ■

Proposition 2 provides a sufficient condition for the the human-inspired holonomic algebraic curves to have robust relative degree at the singular points during a walking gait cycle. Under such robust relative degree property at singular points, it is possible to design tracking control laws for the entire gait cycle using various methodologies, such as the one proposed in [21]. For instance, the output nonlinear tracking controllers in [21] switch between approximate tracking laws close to the singularities, and exact tracking laws away from the singularities. In the final step of the design, a backstepping procedure needs to be employed in order to compute the input v to the integrator given by (19) for generating the proper torque input u that is required to be applied to the knee joint. Finally, we remark that as long as the human hip joint acceleration is bounded, there is no need for measuring it. Because the output tracking control laws, if properly designed, will guarantee boundedness of the tracking errors in the presence of uncertainties and disturbances [31]. Designing output nonlinear tracking controllers for human-inspired algebraic outputs for wearable robots remains the subject of a future work.

CONCLUDING REMARKS AND FUTURE RESEARCH DIRECTIONS

In this article we employed algebraic curves to represent human walking gait data. Using the numerically stable 3L fitting algorithm from the pattern recognition literature, we fitted algebraic curves to human walking gait profiles. We presented conditions by which the generated curves satisfy a robust relative degree condition throughout the human walking gait cycle. The presented material opens up three potential research directions. First, the human-inspired algebraic curves can be employed for designing nonlinear output tracking control schemes for the entire gait cycle of powered prostheses/orthoses. Second, algebraic invariants associated with the human-inspired algebraic curves *might* provide means for gait pathology assessment and classification. Third, the 3L fitting algorithm or its extensions *might* be employed for fitting trivariate (of three variables) implicit polynomials to hip-knee-ankle human walking data.

ACKNOWLEDGMENT

This work was supported by the National Institute of Child Health & Human Development of the NIH under Award Number DP2HD080349. The content is solely the responsibility of the authors and does not necessarily represent the official views of the NIH. Robert D. Gregg, IV, Ph.D., holds a Career Award at the Scientific Interface from the Burroughs Wellcome Fund.

REFERENCES

[1] Gregg, R. D., Lenzi, T., Hargrove, L. J., and Sensinger, J. W., 2014. "Virtual constraint control of a powered prosthetic leg: From simulation to experiments with transfemoral amputees". *IEEE Transactions on Robotics,* ***30***(6), pp. 1455–1471.

[2] Villarreal, D. J., Poonawala, H. A., and Gregg, R. D., 2017. "A robust parameterization of human gait patterns across phase-shifting perturbations". *IEEE Transactions on Neural Systems and Rehabilitation Engineering,* ***25***(3), pp. 265–278.

[3] Holgate, M. A., Sugar, T. G., and Bohler, A. W., 2009. "A novel control algorithm for wearable robotics using phase plane invariants". In Proceedings of 2009 IEEE International Conference on Robotics and Automation (ICRA), pp. 3845–3850.

[4] Quintero, D., Villarreal, D. J., Lambert, D. J., Kapp, S., and Gregg, R. D., 2018. "Continuous-phase control of a powered knee–ankle prosthesis: Amputee experiments across speeds and inclines". *IEEE Transactions on Robotics,* ***34***(3), pp. 686–701.

[5] Quintero, D., Villarreal, D. J., and Gregg, R. D., 2016. "Preliminary experiments with a unified controller for a powered knee-ankle prosthetic leg across walking speeds".

In Proceedings of 2016 IEEE/RSJ International Conference on Intelligent Robots and Systems (IROS), pp. 5427–5433.

[6] Shultz, A. H., and Goldfarb, M., 2018. "A unified controller for walking on even and uneven terrain with a powered ankle prosthesis". *IEEE Transactions on Neural Systems and Rehabilitation Engineering,* ***26***(4), pp. 788–797.

[7] Quintero, D., Martin, A. E., and Gregg, R. D., 2018. "Toward unified control of a powered prosthetic leg: A simulation study". *IEEE Transactions on Control Systems Technology,* ***26***(1), pp. 305–312.

[8] Villarreal, D. J., Quintero, D., and Gregg, R. D., 2017. "Piecewise and unified phase variables in the control of a powered prosthetic leg". In Proceedings of 2017 International Conference on Rehabilitation Robotics (ICORR), pp. 1425–1430.

[9] Sup, F., Bohara, A., and Goldfarb, M., 2008. "Design and control of a powered transfemoral prosthesis". *The International Journal of Robotics Research,* ***27***(2), pp. 263–273.

[10] Liu, M., Zhang, F., Datseris, P., and Huang, H. H., 2014. "Improving finite state impedance control of active-transfemoral prosthesis using dempster-shafer based state transition rules". *Journal of Intelligent & Robotic Systems,* ***76***(3-4), pp. 461–474.

[11] Zhang, F., Liu, M., and Huang, H., 2015. "Investigation of timing to switch control mode in powered knee prostheses during task transitions". *PLOS One,* ***10***(7), p. e0133965.

[12] Zhang, F., Liu, M., and Huang, H., 2015. "Effects of locomotion mode recognition errors on volitional control of powered above-knee prostheses". *IEEE Transactions on Neural Systems and Rehabilitation Engineering,* ***23***(1), pp. 64–72.

[13] Simon, A. M., Ingraham, K. A., Fey, N. P., Finucane, S. B., Lipschutz, R. D., Young, A. J., and Hargrove, L. J., 2014. "Configuring a powered knee and ankle prosthesis for transfemoral amputees within five specific ambulation modes". *PloS One,* ***9***(6), p. e99387.

[14] Martin, A. E., and Gregg, R. D., 2017. "Stable, robust hybrid zero dynamics control of powered lower-limb prostheses". *IEEE Transactions on Automatic Control,* ***62***(8), pp. 3930–3942.

[15] Quintero, D., Lambert, D. J., Villarreal, D. J., and Gregg, R. D., 2017. "Real-time continuous gait phase and speed estimation from a single sensor". In Proceedings of 2017 IEEE Conference on Control Technology and Applications (CCTA), pp. 847–852.

[16] Mohammadi, A., Horn, J., and Gregg, R. D., 2017. "Removing phase variables from biped robot parametric gaits". In Proceedings of 2017 IEEE Conference on Control Technology and Applications (CCTA), pp. 834–840.

[17] Vallery, H., Duschau-Wicke, A., and Riener, R., 2009. "Generalized elasticities improve patient-cooperative control of rehabilitation robots". In Proceedings of 2009 IEEE International Conference on Rehabilitation Robotics (ICORR), pp. 535–541.

[18] Martínez, A., Lawson, B., and Goldfarb, M., 2018. "A controller for guiding leg movement during overground walking with a lower limb exoskeleton". *IEEE Transactions on Robotics,* ***34***(1), pp. 183–193.

[19] Blane, M. M., Lei, Z., Çivi, H., and Cooper, D. B., 2000. "The 3L algorithm for fitting implicit polynomial curves and surfaces to data". *IEEE Transactions on Pattern Analysis and Machine Intelligence,* ***22***(3), pp. 298–313.

[20] Hauser, J., Sastry, S., and Kokotovic, P., 1992. "Nonlinear control via approximate input-output linearization: The ball and beam example". *IEEE Transactions on Automatic Control,* ***37***(3), pp. 392–398.

[21] Tomlin, C., and Sastry, S. S., 1998. "Switching through singularities". *Systems & Control Letters,* ***35***(3), pp. 145–154.

[22] Winter, D. A., 1991. *Biomechanics and motor control of human gait: normal, elderly and pathological*, 2nd ed. University of Waterloo Press.

[23] Marsh, D., 2006. *Applied geometry for computer graphics and CAD*. Springer Science & Business Media.

[24] Silverman, J. H., 2009. *The arithmetic of elliptic curves*, Vol. 106. Springer Science & Business Media.

[25] Unel, M., and Wolovich, W. A., 2000. "On the construction of complete sets of geometric invariants for algebraic curves". *Advances in Applied Mathematics,* ***24***(1), pp. 65–87.

[26] Lei, Z., Blane, M. M., and Cooper, D. B., 1996. "3L fitting of higher degree implicit polynomials". In Proceedings of the 3rd IEEE Workshop on Applications of Computer Vision (WACV), pp. 148–153.

[27] Wolovich, W., Albakri, H., and Yalcin, H., 2002. "The precise measurement of free-form surfaces". *ASME Journal of Manufacturing Science and Engineering,* ***124***(2), pp. 326–332.

[28] Wolovich, W. A., 2001. "On the structure of algebraic curves and their relation to dynamical systems". *IFAC Proceedings Volumes,* ***34***(13), pp. 13–19.

[29] Do Carmo, M. P., 2016. *Differential Geometry of Curves and Surfaces: Revised and Updated Second Edition*. Courier Dover Publications.

[30] Isidori, A., 1995. *Nonlinear Control Systems*, 3rd ed. Springer-Verlag London.

[31] Behtash, S., 1990. "Robust output tracking for nonlinear systems". *International Journal of Control,* ***51***(6), pp. 1381–1407.